

# Catalyzed $\beta$ scission of a carbenium ion — Mechanistic differences from varying catalyst basicity

Qingbin Li and Allan L.L. East

**Abstract:** The  $\beta$ -scission mechanism of physisorbed and chemisorbed pentenium ions, as catalyzed by  $\text{AlH}_2(\text{OH})_2^-$  and by  $\text{AlHCl}_3^-$  anions, was investigated using density functional theory computations and explicit-contact modelling. A thorough search of intermediates was performed for each catalyst. On the aluminum chloride,  $\beta$  scission of an aliphatic, secondary carbenium ion featured chemisorbed and physisorbed ion intermediates, while on the aluminum hydroxide,  $\beta$  scission featured chemisorbed ions but physisorbed *neutral* species. The importance of this work is its demonstration of a qualitatively different mechanism, with qualitatively different intermediates, due only to the different basicity of the two catalysts.

*Key words:* C—C bond fission,  $\beta$  scission, carbenium ion, catalysis, mechanism.

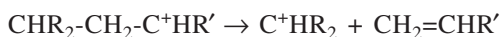
**Résumé :** Faisant appel à la méthode de calculs de la théorie de la densité fonctionnelle et à la modélisation par contacts explicites, on a étudié le mécanisme de la scission  $\beta$  d'ions penténium physisorbés et chimisorbés, tel que catalysée par les anions  $\text{AlH}_2(\text{OH})_2^-$  et  $\text{AlHCl}_3^-$ . Pour chacun des catalyseurs, on a fait une étude approfondie des intermédiaires. Sur le chlorure d'aluminium, la scission  $\beta$  d'un ion carbénium secondaire et aliphatique implique des intermédiaires ioniques chimisorbés et physisorbés alors que sur l'hydroxyde d'aluminium, la scission  $\beta$  implique des ions chimisorbés, mais des espèces neutres physisorbées. L'importance de ce travail est de démontrer que, en raison seulement de différences dans les basicités des deux catalyseurs, que les réactions impliquent des mécanismes qualitativement différents avec des intermédiaires qualitativement différents.

*Mots clés :* fission d'une liaison C—C, scission  $\beta$ , ion carbénium, catalyse, mécanisme.

[Traduit par la Rédaction]

## Introduction

Alkane cracking can be catalyzed by solid zeolites (aluminosilicates), chloroaluminate ionic liquids (1), and liquid superacids (2) such as  $\text{HF}\cdot\text{SbF}_5$  and  $\text{HSO}_3\text{F}\cdot\text{SbF}_5$  (having a great deal of ionic-liquid character). The cracking is generally performed by carbenium ions in a chain reaction (3), where the first step is hydride abstraction by a little carbenium ion to make a big carbenium ion, and the second step is  $\beta$  scission of the big carbenium ion, e.g.,



to create another little carbenium ion. The net result is cracking of the big alkane.

Upon closer scrutiny, the mechanism of the  $\beta$ -scission step must be different for different catalysts. From product distribution studies, several scientists (3–7) suggested that carbenium ion chemistry as observed in liquid superacids could be applied to the reactions on zeolites, although the

product distributions were generally different. However, the direct comparison to liquid superacid chemistry was called into question by both experimental studies (8, 9) and theoretical computations (10, 11), which suggested that bound alkoxy groups (chemisorbed carbenium ions), rather than labile (physisorbed) carbenium ions, are the intermediates on zeolite surfaces (12, 13).

The success of those initial computations, combined with the belief that the differences may be due to large structural physical effects of the zeolite, pushed some computational chemists into invoking “large-scale” computational modelling in which the number of atoms in the calculation is maximized by invoking further computational approximations. Currently, however, this field is still in its infancy, limited in its accuracy by the approximations required to do large-scale modelling. A good example of this is the work of Demuth et al. (14), who modelled the isomerization of 2-pentene (actually, chemisorbed 2-pentenium ion to chemisorbed 2-methyl-1-butenium ion) in a ZSM-22 zeolite with a large-scale simulation, invoking periodic boundary conditions, the PW91 exchange functional, a plane-wave basis set, and approximate transition states. Their computations produced a physisorbed carbenium ion that would be observably stable, with barriers of 8 kcal mol<sup>-1</sup> for chemisorption and 18 kcal mol<sup>-1</sup> for proton transfer to the catalyst (1 cal = 4.184 J). This is in complete disagreement with in situ magic-angle-spinning nuclear magnetic resonance (MAS NMR) studies,

Received 3 May 2005. Published on the NRC Research Press Web site at <http://canjchem.nrc.ca> on 21 September 2005.

**Q. Li and A.L.L. East.**<sup>1</sup> Department of Chemistry and Biochemistry, University of Regina, Regina, SK S4S 0A2, Canada.

<sup>1</sup>Corresponding author (e-mail: [Allan.East@uregina.ca](mailto:Allan.East@uregina.ca)).

in which physisorbed nonaromatic carbenium ions have been eagerly searched for but never found (9, 15–22).

Despite the limitations on large-scale computational modelling, quantum chemical calculations are still a powerful tool in studying and understanding these molecular mechanisms. For example, the effect of the relative acidity or basicity of the catalyst upon the mechanism can be studied, without the need to invoke large-scale modelling. In 2003, our group published a theoretical study on an idealized Bronsted acid catalytic cycle for  $C_6H_{14} \rightarrow C_3H_8 + C_3H_6$ , using small cationic Bronsted acids in the computations (23). There we demonstrated that the existence of certain intermediates varied with the catalyst, simply because of the acidity of the catalyst. Here, we are going to show that varying catalyst basicity can change the catalyzed  $\beta$ -scission mechanism of  $C_5H_{11}^+ \rightarrow C_2H_5^+ + C_3H_6$ .

Modelling real systems is not a goal of this paper. If large-scale computational modelling of zeolites and ionic liquids could be achieved, and the results demonstrated a difference in mechanism, we would likely still be unable to state which aspect of the two catalysts is the most important one responsible for the mechanism change. Fundamental studies are required, and this is one of them. Also, we are certainly not suggesting that the change in relative basicity is the only reason for the mechanism change between zeolites and ionic liquids. We are simply providing the extremely important demonstration that relative catalyst basicity can be responsible for qualitative changes in the  $\beta$ -scission mechanism.

This paper is a computational chemistry study of the mechanisms, i.e., minimum energy pathways, used by the aluminum chloride  $AlHCl_3^-$  and the aluminum hydroxide  $AlH_2(OH)_2^-$  in performing the  $\beta$  scission of 2-pentenium ion into ethenium ion and propene. All the pathways start and end with covalently bound (chemisorbed) ion–catalyst complexes, as influenced by the  $\beta$ -scission study by Frash et al. (FKRS) (24). The initial purpose was to investigate the  $\beta$  scission with  $AlHCl_3^-$  and compare these results to the results of FKRS who used  $AlH_2(OH)_2^-$ . However, it was soon discovered that the potential energy surface for the reaction on  $AlH_2(OH)_2^-$  is even more complex than those reported by FKRS, and a direct comparison required a thorough investigation with one carbenium ion (2-pentenium ion), one level of theory (B3LYP/6-31G(d,p)), and the two catalyst fragments. We will compare our results with the other published computational studies of cationic  $\beta$  scission, which are the  $\beta$ -scission papers of FKRS (24) and Hay et al. (25), and the reverse  $\beta$ -scission (oligomerization) paper of Svelle et al. (26).

This paper is not addressed solely to those interested in the effects of varying the basicity of a catalyst. We hope it is also of interest to organic chemists interested in catalysis at the molecular level, and to surface scientists interested in the nature of physisorbed and chemisorbed states (27) on compound surfaces like metal oxides.

## Methods, models, and terminology

All calculations used the semi-empirical density functional theory model called B3LYP (28, 29) with the 6-

31G(d,p) orbital basis set (30). Molecular geometries and harmonic frequencies for intermediates and transition states were computed using analytic first and second derivative formulae, as are routine with most quantum chemistry codes. All reported results come from calculations with the GAUSSIAN 98 software suite (30) using the default numerical grid. In most cases, the PQS 3.0 software suite (31) was used to speed up transition-state searches because of its parallelism and because the Baker eigenvector-following algorithm (32) is not restricted to 50 variables, as it is in GAUSSIAN 98. However, because the default grid in PQS 3.0 is finer, the B3LYP energies between the two codes are not compatible, and final results were run with GAUSSIAN 98. The energies reported are not corrected for zero-point vibrational energies or thermal corrections, primarily to maintain focus on the underlying (and complicated) potential energy surface (PES).

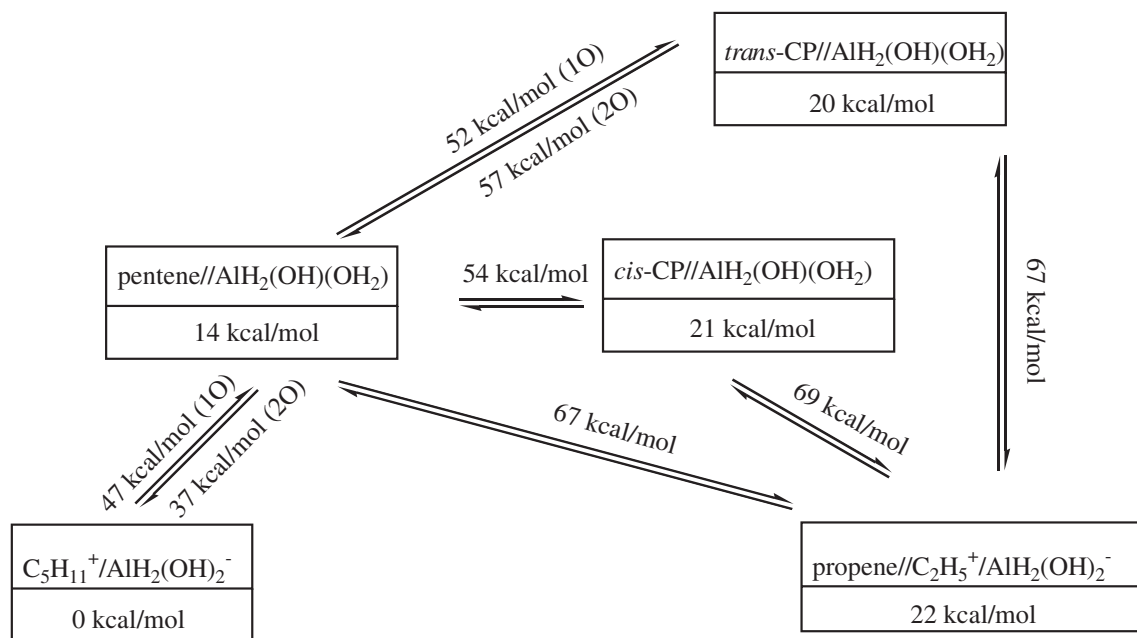
Explicit-contact modelling was used with small catalysts. The catalysts are small for several reasons. First, this study required thorough searches of two tricky potential energy surfaces, so we wanted to compute real transition states in full-coordinate space (63 and 57 degrees of freedom, respectively), and properly verify each one by following the connections from these to the intermediates on either side; this cannot be done with larger catalyst models. Second, the 1998 FKRS study (24) with pentenium ion and  $AlH_2(OH)_2^-$  was incomplete, and we wished to make use of the stationary points they had. Third, the  $AlHCl_3^-$  catalyst was chosen from our exploratory ionic liquid calculations (33), which suggest that the active  $Al_2Cl_7^-$  Lewis acid anion (34, 35) will create  $AlHCl_3^-$  upon hydride abstraction from an alkane.

We will use the word chemisorbed to describe states in which there is a covalent bond between catalyst and reactant; this refers to states that have been variously called alkoxy,  $\sigma$  bonded, or alkyl silyl ether. We will use the word physisorbed to describe van der Waals neutral-pair complexes of catalyst and reactant, but also ion-pair (cation–anion, or sometimes called “zwitterionic”) complexes. Some ion-pair complexes have an ionic bond strong enough to be considered chemisorbed, but in our systems the dissociation energies are much smaller because a proton transfer would occur if the molecular ions were pulled apart, resulting in neutral dissociated molecules. Although the concepts of chemisorbed and physisorbed states are taken from surface-science terminology (27), we think these states may prove to be pervasive in homogeneous as well as heterogeneous catalysis. We will use single and double slashes to denote chemisorbed and physisorbed complexes, respectively (e.g.,  $C_5H_{11}^+/AlHCl_3^-$  vs.  $C_5H_{11}^+//AlHCl_3^-$ ). We will refer to the conversion from chemisorbed to physisorbed as ascension, and the opposite as descension, since the terms desorption and adsorption strictly refer to molecules leaving and approaching the surface.<sup>2</sup>

For most stationary points, there is more than one possible orientation of the reactant relative to the catalyst, and many possibilities were investigated. These possibilities are usually indistinguishable in energy on the scale of the reaction pathway, as will be demonstrated. Our atom-numbering con-

<sup>2</sup>R.A. Wolkow and G.P. Lopinski. Private communication. 2004.

**Scheme 1.** Overview of the B3LYP/6-31G(d,p) potential energy surface for the  $\beta$  scission of 2-pentenium ion on the  $\text{AlH}_2(\text{OH})_2^-$  catalyst fragment. Notation: chemisorbed (/), physisorbed (//), dimethylcyclopropane (CP). Transition-state energies are listed as well, including two values in cases where two distinct paths were found for the same step in the mechanism.



vention will be to count the carbon atoms as C1, C2, C3, C4, and C5, such that the C2 atom is initially bound to the O1 or C11 atom of the catalyst in the chemisorbed state.

The transition states that were located had only one imaginary vibrational frequency corresponding to the desired reaction coordinate. Each transition state was validated by two verification minimizations (to locate the two relevant intermediates) from displaced geometries on either side of the transition state. The displaced geometries for these verification runs were obtained by identifying the key internal coordinates in the crucial normal mode via the animation of the imaginary frequency, and then displacing these coordinates in both directions (minus or plus 0.03 Å for bond lengths; minus or plus 3° for angles and dihedrals).

Finally, we define some abbreviations for the rest of the article: potential energy surface (PES), dimethylcyclopropane (CP), protonated dimethylcyclopropane (PCP) (the prevalent form of a poorly solvated or gas-phase 2-pentenium ion).

## Results

### $\text{AlH}_2(\text{OH})_2^-$ catalyst

Scheme 1 shows an overview of the results for the  $\beta$  scission of a chemisorbed 2-pentenium ion on  $\text{AlH}_2(\text{OH})_2^-$ , to form a chemisorbed ethenium ion and a physisorbed propene. The only first step we could find is ascension to a physisorbed, neutral 1-pentene. After ascension, the physisorbed 1-pentene was found to be able to produce the intended products via more than one path. The direct one is Bronsted acid catalyzed  $\beta$  scission; the indirect paths involve Bronsted acid catalyzed isomerization of physisorbed 1-pentene to physisorbed *cis*- or *trans*-CP, followed by Bronsted acid catalyzed fission of two simultaneous C—C bonds. FKRS had presented the transition state for only the

second step of one of the indirect routes (24); we believe it is the step from *trans*-CP to products.

On this PES, all the physisorbed intermediate states are neutral-pair complexes. For the various transition states, there are varying degrees of charge separation between catalyst and reactant, as caused by proton transfer. Also, as FKRS had found (24), direct  $\beta$  scission from a chemisorbed state is not a minimum energy pathway on this PES. We now describe the various steps on this PES in more detail.

### Ascension step

Figure 1 shows the 3D images of the stationary-point geometries for three different versions of the ascension of 2-pentenium to 1-pentene on  $\text{AlH}_2(\text{OH})_2^-$ . Figure 2 has sketches of the transition states that demonstrate the bond rearrangement mechanism. Table 1 provides some geometric data for the nine structures of Fig. 1 using the atom numbering of Fig. 2.

All three transition states feature partial ascension of the pentenium cation, as well as partial proton transfer from it to the catalyst anion to avoid the creation of an ion pair. In the top row path, the transferring proton goes from C1 to O1 (the single oxygen pathway, Fig. 2a), while in the other two paths the proton goes from C1 to O2 (the two oxygen pathways, Fig. 2b), and all three paths result in the coordination of the newly formed OH bond of the catalyst to the pentene double bond. The involvement of the second oxygen atom lowers the barrier height from 47 to 37 kcal mol<sup>-1</sup>.

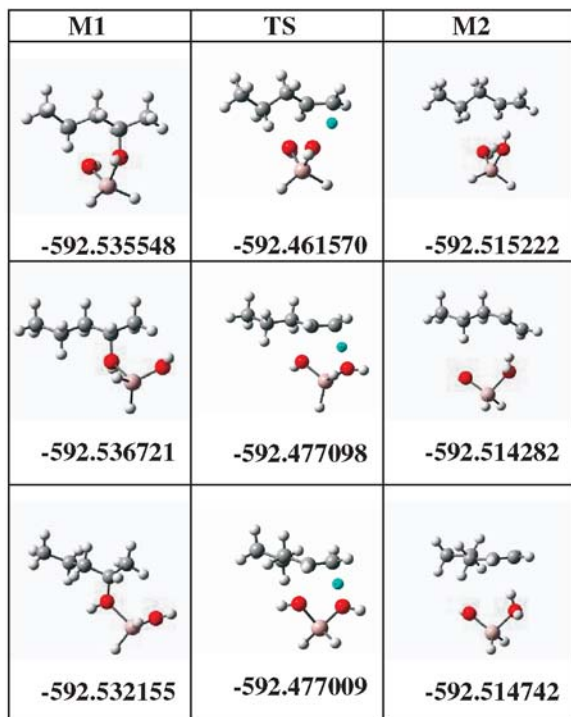
The lower two paths in Fig. 1 only differ by the conformer of the hydrocarbon; the middle path produces a *gauche* alkene from an all-*trans* alkoxy species, while the bottom path in the figure produces a *cis*-alkene from a *gauche* alkoxy species. While the lower two pathways are isoenergetic with this model fragment, a truer zeolite surface would probably make *gauche* alkoxy forms more favoured

**Table 1.** Selected geometry parameters (Å and °) for three different ascension paths with a zeolite fragment.<sup>a</sup>

	M1	TS	M2	M1	TS	M2	M1	TS	M2
	1O from trans			2O from trans			2O from gauche		
<b>Bond lengths (Å)</b>									
C1—C2	1.521	1.417	1.340	1.522	1.407	1.340	1.521	1.409	1.341
C2—C3	1.527	1.469	1.503	1.527	1.500	1.502	1.530	1.499	1.503
C3—C4	1.536	1.541	1.542	1.534	1.533	1.541	1.536	1.536	1.531
C2—C4	2.585	2.542	2.540	2.575	2.580	2.549	2.605	2.581	2.576
O1—C2	1.476	2.505	3.189	1.473	2.150	4.356	1.478	2.135	3.774
C1—H1	1.093	1.181	2.239	1.093	1.324	2.179	1.092	1.304	2.183
O1—H1	2.645	1.664	0.985	2.640	2.534	2.983	2.580	2.512	2.830
O2—H1	4.470	3.332	2.849	2.467	1.300	0.983	2.532	1.324	0.986
O2—H2	2.475	1.859	2.460	3.350	3.684	3.620	3.792	3.821	3.576
<b>Bond angles (°)</b>									
C2—C3—C4	115.1	115.2	113.1	114.6	116.6	113.8	116.3	116.5	116.2
C1—C2—C3—C4	179.1	140.1	121.3	-176.1	175.7	124.9	57.5	40.6	-2.7
C2—C3—C4—C5	173.3	175.5	173.6	-179.6	176.5	174.9	175.9	180.0	-179.2
C2—C1—H1	110.7	87.1	73.4	109.7	104.7	84.4	109.9	104.4	80.3

<sup>a</sup>Corresponds to the images of Fig. 1 with the atom numbering of Fig. 2. TS = transition state between two minima (M1, M2).

**Fig. 1.** B3LYP/6-31G(d,p) stationary points for three different ascension paths of 2-pentenium ion to pentene on  $\text{AlH}_2(\text{OH})_2^-$ . The blue hydrogen is the one transferring from the pentenium ion to the catalyst. Top row: a one oxygen path. Middle row: a two oxygen path from a *trans*-pentenium ion form. Bottom row: a two oxygen path from a *gauche*-pentenium ion form.

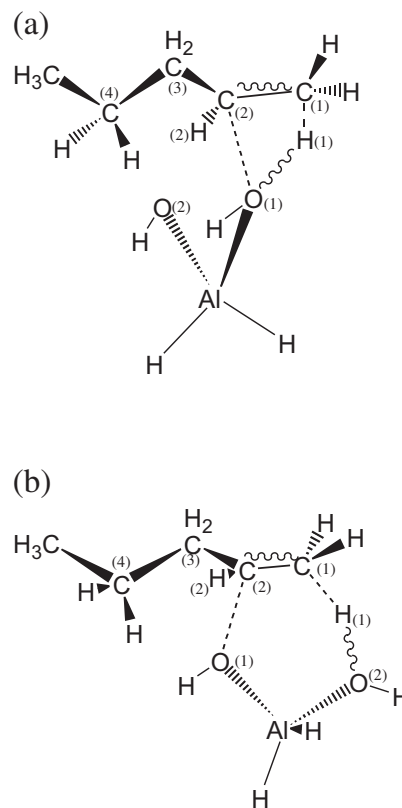


than all-trans ones. Paths involving other conformers may also exist.

### Cyclization step

Figure 3 shows the 3D images of the geometries for three different versions of the isomerization of 1-pentene to CP on  $\text{AlH}_2(\text{OH})_2^-$ . Figure 4 has sketches of the transition states that demonstrate the bond rearrangement mechanism. Ta-

**Fig. 2.** Transition-state sketches for the ascension paths of 2-pentenium ion to pentene on  $\text{AlH}_2(\text{OH})_2^-$ : (a) the single oxygen pathway; (b) the two oxygen pathways. The dashed lines indicate bonds in the reactant, while the squiggly lines indicate bonds in the product.



ble 2 provides some geometric data for the nine structures of Fig. 3 using the atom numbering of Fig. 4.

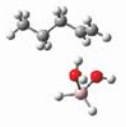
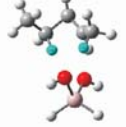
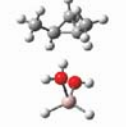
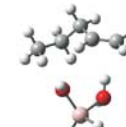
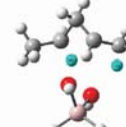
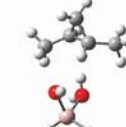
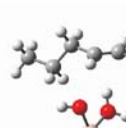
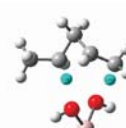
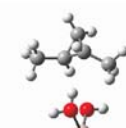
All three paths involve an ion-pair transition state in which the proton H1 has returned to C1 from the catalyst. However, to finish forming the cyclized intermediate, the proton H4 returns to the catalyst from C4, making this a

**Table 2.** Selected geometry parameters (Å and °) for three different isomerization paths with a zeolite fragment.<sup>a</sup>

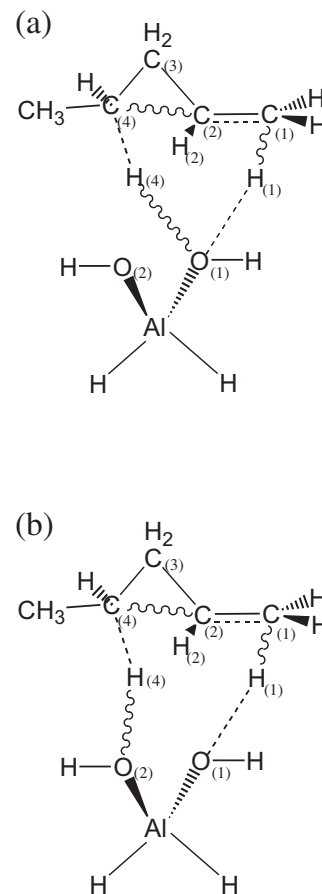
	M1	TS	M2	M1	TS	M2	M1	TS	M2
	1O forming <i>cis</i> -CP			1O forming <i>trans</i> -CP			2O forming <i>trans</i> -CP		
<b>Bond lengths (Å)</b>									
C1—C2	1.341	1.463	1.516	1.341	1.463	1.517	1.340	1.462	1.519
C2—C3	1.503	1.427	1.507	1.504	1.425	1.508	1.504	1.440	1.507
C3—C4	1.541	1.627	1.508	1.544	1.633	1.506	1.542	1.584	1.508
C2—C4	2.542	2.088	1.540	2.566	2.100	1.535	2.538	1.972	1.536
O1—C2	3.213	3.050	3.139	3.219	3.050	3.124	3.226	3.483	3.995
C1—H1	2.214	1.112	1.096	2.191	1.112	1.096	2.289	1.140	1.094
O1—H1	0.986	2.006	3.036	0.986	2.003	2.863	0.985	1.756	2.936
C4—H4	1.097	1.118	2.239	1.099	1.115	2.420	1.096	1.159	2.232
O1—H4	3.184	1.996	0.982	3.327	2.036	0.979			
O2—H2	2.407	1.764	2.628	2.456	1.800	2.487			
O2—H4							2.868	1.720	0.979
O2—C4							3.728	2.869	3.167
C2—H4	2.796	2.02	2.197	2.804	2.037	2.181	2.701	1.897	2.360
<b>Bond angles (°)</b>									
C2—C3—C4	113.3	86.0	61.4	114.7	86.5	61.2	112.9	81.3	61.3
C1—C2—C3—C4	-121.7	-92.4	-113.0	126.0	94.7	110.6	117.9	96.7	112.3
C2—C3—C4—C5	-176.8	120.9	113.0	65.2	114.3	112.4	172.6	125.2	110.9
C2—C1—H1	76.0	105.1	111.9	76.6	105.2	112.3	72.2	108.2	110.8

<sup>a</sup>Corresponds to the images of Fig. 3 with the atom numbering of Fig. 4.

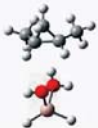

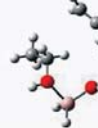
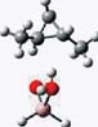


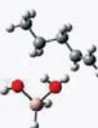
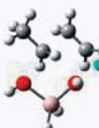
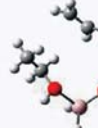
**Fig. 3.** B3LYP/6-31G(d,p) stationary points for three different isomerization paths of pentene on  $\text{AlH}_2(\text{OH})_2^-$ . The blue hydrogens are the ones transferring between the hydrocarbon and the catalyst. Top row: a one oxygen path forming *cis*-dimethylpropane. Middle row: a one oxygen path forming *trans*-dimethylpropane. Bottom row: a two oxygen path forming *trans*-dimethylpropane.

M1	TS	M2
 -592.514331	 -592.450282	 -592.503220
 -592.514952	 -592.453145	 -592.504439
 -592.514748	 -592.446308	 -592.504103

**Fig. 4.** Transition-state sketches for the isomerizations of pentene on  $\text{AlH}_2(\text{OH})_2^-$ : (a) the single oxygen pathways; (b) the two oxygen pathway. The dashed lines indicate bonds in the reactant, while the squiggly lines indicate bonds in the product.



**Fig. 5.** B3LYP/6-31G(d,p) stationary points for three different scission (cracking) reactions on  $\text{AlH}_2(\text{OH})_2^-$ . The blue hydrogen is the one transferring from the catalyst to the hydrocarbon. Top row: scission of *cis*-dimethylpropane. Middle row: scission of *trans*-dimethylpropane. Bottom row: scission of 1-pentene.

M1	TS	M2
 -592.503225	 -592.426301	 -592.500980
 -592.504103	 -592.429541	 -592.501223
 -592.515471	 -592.429249	 -592.501570

double-proton transfer step. The top two paths in the figure are single oxygen pathways (Fig. 4a) in which departing and incoming protons use the same oxygen atom, while the bottom path is a two oxygen pathway (Fig. 4b). All three paths result in a newly formed OH bond on the catalyst that coordinates to the region of the two tertiary carbons C2 and C4. Unlike in the ascension step, the two oxygen path has a higher barrier than the single oxygen paths in the cyclization step, although the difference here is smaller (43 vs. 38 kcal mol<sup>-1</sup>).

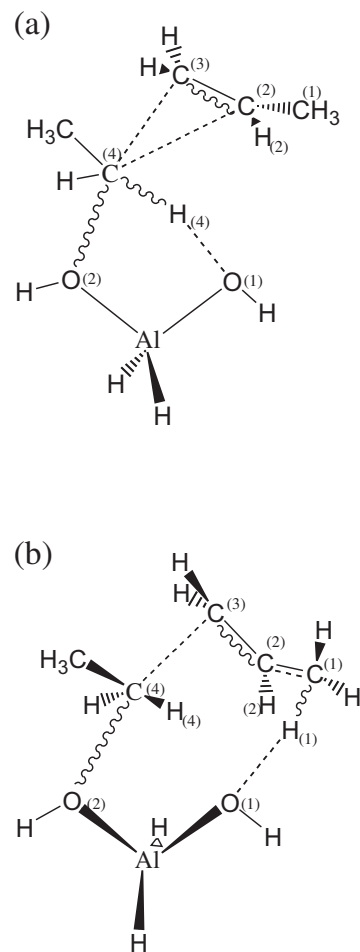
The two upper paths in Fig. 3 only differ by the conformation; the top path forms *cis*-CP from a *trans*-gauche pentene, while the middle path forms *trans*-CP from all-gauche pentene. Since our two oxygen pathway produced *trans*-CP, this model fragment might also produce a two oxygen pathway that forms *cis*-CP.

#### Scission step

Figure 5 shows the 3D images of the stationary points for three different versions of the scission step that produces chemisorbed ethenium ion and physisorbed propene. Figure 6 has sketches of the transition states that demonstrate the bond rearrangement mechanism. Table 3 provides some geometric data for the nine structures of Fig. 5, using the atom numbering of Fig. 6.

All three paths involve a transition state in which a proton has transferred from a catalyst oxygen to the hydrocarbon, and the C4 atom has migrated in an S<sub>N</sub>2-like fashion between C3 and a second catalyst oxygen (all two oxygen pathways). In the upper two versions in Fig. 5, products are

**Fig. 6.** Transition-state sketches for the scission (cracking) steps on  $\text{AlH}_2(\text{OH})_2^-$ : (a) the dimethylcyclopropane pathways; (b) the pentene pathway. The dashed lines indicate bonds in the reactant, while the squiggly lines indicate bonds in the product.



created from CP (Fig. 6a), and all the action happens at the C4 atom; it sheds its bonds to C2 and C3 and creates bonds to the Bronsted proton and a catalyst oxygen. The bottom path creates the products directly from pentene (Fig. 6b) by transferring the catalytic proton to C1, and allowing the C4 atom to break its bond to C3 and form its bond to the catalyst. The three transition states are very isoenergetic, lying in a 69–72 kcal mol<sup>-1</sup> range relative to the products.

The two upper paths in Fig. 5 only differ by conformation; the top path starts with *cis*-CP, while the middle path starts with *trans*-CP. The three versions of the products appearing in Fig. 6 represent three different orientations of the ethyl and propene groups on the catalyst.

#### $\text{AlHCl}_3^-$ catalyst

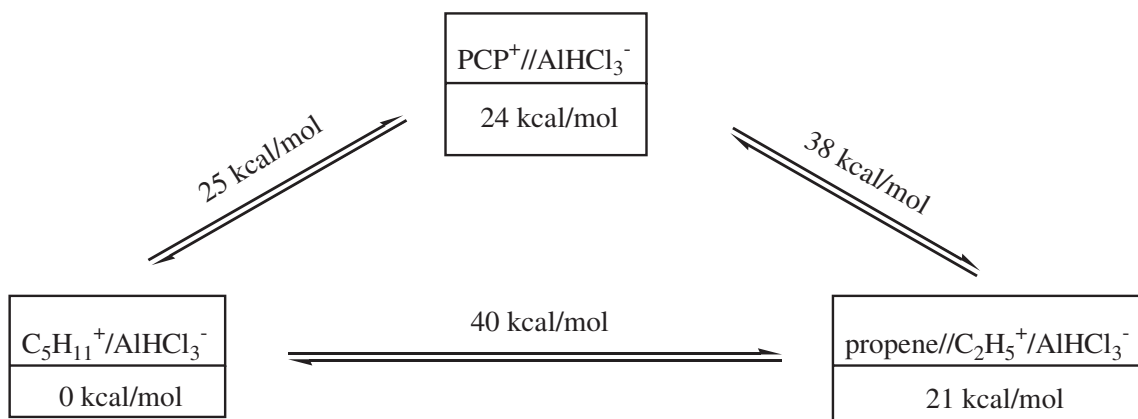
Scheme 2 shows an overview of the results for the same  $\beta$ -scission reaction, but with  $\text{AlHCl}_3^-$  as the catalyst. There are two significant differences between this PES and that from  $\text{AlH}_2(\text{OH})_2^-$  catalysis. One is the absence of minimum energy pathways involving physisorbed neutral-pair intermediates; instead, a barely stable ion-pair intermediate is seen (upper path in Scheme 2), involving a physisorbed, protonated *cis*-PCP. The second difference is that there is a

**Table 3.** Selected geometry parameters (Å and °) for three different scission (cracking) paths with a zeolite fragment.<sup>a</sup>

	M1	TS	M2	M1	TS	M2	M1	TS	M2
	Scission of <i>cis</i> -CP			Scission of <i>trans</i> -CP			Scission of 1-pentene		
<b>Bond lengths (°)</b>									
C1—C2	1.516	1.487	1.501	1.519	1.482	1.500	1.340	1.475	1.500
C2—C3	1.508	1.365	1.335	1.507	1.367	1.336	1.503	1.369	1.336
C3—C4	1.507	2.121	3.976	1.508	2.096	3.944	1.540	2.107	3.937
C2—C4	1.540	2.289	3.922	1.536	2.367	4.024	2.552	2.554	4.021
O1—C2	3.159	3.403	4.029	3.302	3.417	4.070	3.321	3.524	4.058
O1—C4	3.123	2.940	2.591	3.169	2.970	3.802			
C1—H1							2.165	1.115	1.098
O1—H1							0.983	1.991	2.373
C4—H4	2.185	1.094	1.089	2.232	1.092	1.091			
O1—H4	0.983	1.883	2.591	0.979	1.936	3.405			
O2—C4	3.428	2.419	1.465	3.388	2.428	1.462	3.689	2.362	1.462
<b>Bond angles (°)</b>									
C2—C3—C4	61.5	78.8	78.0	61.3	83.4	83.7	114.0	92.0	83.9
C1—C2—C3—C4	112.9	92.8	93.9	112.3	89.6	96.8	-131.8	-90.6	-95.2
C2—C3—C4—C5	-113.0	-118.2	-137.5	110.9	127.3	116.3	-177.8	171.1	152.2

<sup>a</sup>Corresponds to the images of Fig. 5 with the atom numbering of Fig. 6.

**Scheme 2.** Overview of the B3LYP/6-31G(d,p) potential energy surface for the  $\beta$  scission of 2-pentenium ion on the  $\text{AlHCl}_3^-$  catalyst fragment. Notation: chemisorbed (/), physisorbed (//), protonated dimethylcyclopropane (PCP). Transition-state energies are listed as well.



direct one-step  $\beta$ -scission pathway from chemisorbed 2-pentenium ion. Several bombed searches suggest that a *flat, wide energy shelf* for PCP exists for both paths on the PES; PCP is barely stable in the upper pathway and not stable on the lower pathway.

The PES is also fairly flat in the region of neutral pair physisorbed intermediates. Here, the flat PES caused difficulties when using GAUSSIAN 98 frequency runs to verify stationary points because, in a few cases, a low-frequency mode had a frequency below the noise level of the normal mode diagonalization. This appears to be due to the coarse DFT numerical grid; when we switched to the “ultrafine” grid, we were able to definitively find four physisorbed intermediates (two ion pair and two neutral pair), and two transition states for conversion of these neutral-pair ones to ion-pair ones. In Scheme 2, the  $\text{PCP}^+//\text{AlHCl}_3^-$  intermediate sits at 24 kcal mol<sup>-1</sup>; the other three physisorbed minima are at 21 kcal mol<sup>-1</sup> (pentenium<sup>+</sup>), 21 kcal mol<sup>-1</sup> (pentene), and 28 kcal mol<sup>-1</sup> (CP), and the transition states are at 22 kcal

mol<sup>-1</sup> (pentenium<sup>+</sup>  $\rightarrow$  pentene) and 30 kcal mol<sup>-1</sup> ( $\text{PCP}^+ \rightarrow \text{CP}$ ). We are not presenting these results in Scheme 2 because: (i) no paths leading to  $\beta$  scission could be found from these minima; and (ii) they required the ultrafine grid.

In both  $\beta$ -scission pathways in Scheme 2, the hydrogens never leave their respective carbon partners. The C2—C11 and C3—C4 bonds are broken, and a C4—C13 bond is formed (both are two chlorine pathways). The presence of three chlorines in our catalyst model may prevent a *trans*-PCP intermediate from forming vis-à-vis the *cis* form.

#### Ascension step

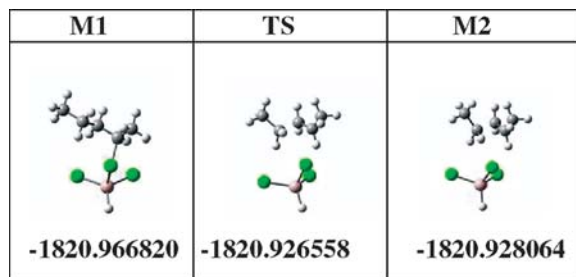
We present only one path for the ascension of 2-pentenium ion on  $\text{AlHCl}_3^-$ ; Fig. 7 shows the 3D images of its stationary-point geometries. Figure 8 has the sketch of the transition state demonstrating the “hydrogen bonds” between catalyst and reactant, and Table 4 provides some geometric data for the three structures of Fig. 7 using the atom numbering of Fig. 8.

**Table 4.** Selected geometry parameters of the ascension of pentenium ion and two different scission (cracking) paths with an ionic liquid fragment.

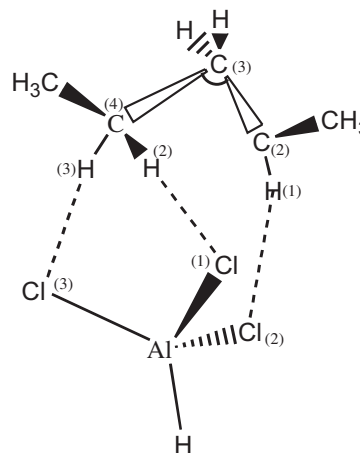
	M1	TS	M2	M1	TS	M2	M1	TS	M2
	Ascension step <sup>a</sup>			Scission of chemisorbed pentenium ion <sup>b</sup>			Scission of physisorbed pentenium ion <sup>b</sup>		
<b>Bond lengths (Å)</b>									
C2—C3	1.523	1.419	1.415	1.415	1.354	1.335	1.522	1.358	1.335
C3—C4	1.533	1.648	1.64	1.638	2.418	3.756	1.534	2.359	3.765
C2—H2	2.867	2.236	1.917	1.910	2.497	3.607	2.853	2.397	3.110
C4—H2	1.097	1.096	1.113	1.114	1.082	1.089	1.096	1.083	1.089
C2—Cl1	1.917	3.306	3.442	3.450	4.046	4.874	1.917	4.163	4.720
C2—Cl2	3.697	3.398	3.411	3.412	3.879	4.299	3.713	5.872	6.370
C4—Cl3	4.710	3.660	3.584	3.578	2.565	1.869	4.846	2.653	1.872
Cl1—H2	3.792	2.946	2.565	2.544	2.770	3.122	2.919	2.539	2.920
Cl2—H1	2.827	2.471	2.523	2.518	2.999	3.497	2.836	5.506	5.954
Cl3—H3	4.399	2.781	2.820	2.798	2.594	2.386	5.832	2.639	2.364
Cl3—Al				2.187	2.275	2.483	2.137	2.268	2.492
<b>Bond angles (°)</b>									
C2-C3-C4	117.0	93.4	80.6	80.3	84.6	78.5	117.0	82.1	83.1
C1-C2-C3-C4	-54.4	-97.0	-96.0	-96.1	-99.0	-96.3	-53.2	-95.4	-90.7
C2-C3-C4-C5	-179.7	141.3	116.5	116.4	146.4	174.2	-179.0	-111.5	-108.0
Cl3-C4-H2				66.8	81.7	103.8			
Cl3-C4-H3				37.9	79.4	104.4			
Al-Cl3-C4				80.5	92.4	103.6	85.4	96.6	106.9

<sup>a</sup>Corresponds to the images of Fig. 7 with the atom numbering of Fig. 8.

<sup>b</sup>Corresponds to the images of Fig. 9 with the atom numbering of Fig. 10.

**Fig. 7.** B3LYP/6-31G(d,p) stationary points for the ascension step found on  $\text{AlHCl}_3^-$ .

The chemisorbed state has a C2—Cl1 distance of 1.9 Å. After ascension, the physisorbed pentenium ion has a structure that some scientists describe as an edge-protonated cyclopropane ring, where the C2, C3, C4, and H2 atoms lie nearly planar, and the C2-C3-C4 angle is acute ( $81^\circ$ ); we refer to it as PCP, to remind the reader of the analogous CP structure in the  $\text{AlH}_2(\text{OH})_2^-$  modelling. The resulting  $\text{C}_5\text{H}_{11}^+/\text{AlHCl}_3^-$  intermediate features three  $\text{H}\cdots\text{Cl}$  interactions in a stool-like structure in which the three catalyst chlorine atoms are coordinated with three different hydrogens near the C-C-C-H ring. These three  $\text{H}\cdots\text{Cl}$  bond distances change from 3.8, 2.8, and 4.4 Å to 2.9, 2.5, and 2.8 Å in the transition state, and finish at 2.6, 2.5, and 2.8 Å in the stool-like structure, respectively. During this procedure, the C4—Cl3 bond distance also decreases from 4.7 to 3.6 Å, thus preparing for tight coordination in the scission step. The transition state for this endothermic step is extremely late, with the C2—Cl1 bond almost completely broken, and the

**Fig. 8.** Transition-state sketch for the ascension of pentenium ion on  $\text{AlHCl}_3^-$ . The dashed lines indicate coordination interactions between Cl and H in the stool-like structure of the ion-pair complex.

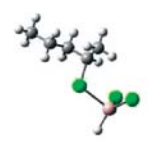
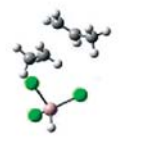
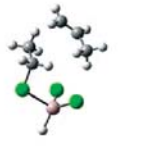
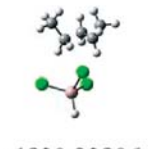
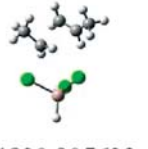
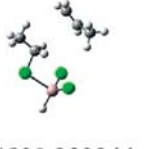
closing of the C2 carbenium site to the C4 atom (actually to the C4—H2 bond) almost complete.

### Scission step

We present two versions of the scission step that produce chemisorbed ethenium ion and physisorbed propene; Fig. 9 shows the 3D images of their stationary-point geometries. Figure 10 has the sketch of the transition states to demonstrate the bond rearrangement mechanism, and Table 4 provides some geometric data for the three structures of Fig. 9 using the atom numbering of Fig. 10.



**Fig. 9.** B3LYP/6-31G(d,p) stationary points for two different scission (cracking) reactions on  $\text{AlHCl}_3^-$ . Top row: one-step  $\beta$  scission of chemisorbed pentenium ion. Bottom row: scission of physisorbed pentenium ion (also called protonated dimethylcyclopropane).

M1	TS	M2
 -1820.966781	 -1820.903667	 -1820.932488
 -1820.928064	 -1820.905623	 -1820.932944

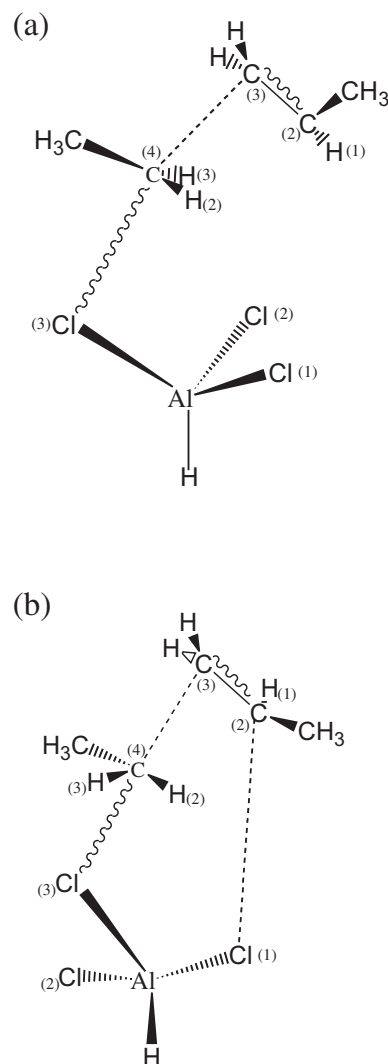
The top row of Fig. 9 shows the path for  $\beta$  scission directly from the chemisorbed pentenium ion, and the bottom row is the scission from the precariously stable PCP ion. Both go through very similar scission transition states in which the migrating C4 atom has moved to a spot roughly equidistant between the C3 atom it was leaving (2.4 Å) and the Cl3 atom it was approaching (2.6–2.7 Å). The C1—C2 bond changes from a single bond (1.41 Å) through the transition state (1.35 Å) to a double bond (1.33 Å). The products from these two scission-step versions differ in orientation of the ethyl and propene units relative to the catalyst, but are otherwise identical chemically.

## Discussion

### Visualizing and comparing the two catalyst mechanisms

The PES energetics are key to understanding the apparently dramatic qualitative differences in the  $\beta$ -scission mechanism on  $\text{AlHCl}_3^-$  vs.  $\text{AlH}_2(\text{OH})_2^-$ . To do this comparison, we chose to sketch approximate contour plots of the PES for both catalysts (Figs. 11 and 12), oriented in a common way that includes both neutral-pair and ion-pair physisorbed regions in both plots. The contours are approximate, based only on the 11 and six stationary points, respectively, of the lowest-energy paths between regions, but also guided by the nonexistence of other stationary points. For both these plots, the horizontal coordinate is a crude coordinate representing the general stepwise reaction path of ascension, isomerization, and  $\beta$  scission, and the vertical coordinate represents the ion-pair vs. neutral-pair nature of the physisorbed complexes (ion pair on the bottom, neutral pair on the top). The layout of this plot is rather arbitrary, but we have chosen to put the physisorbed pentene and 2-pentenium regions to the left of the CP and PCP ones because they require less geometrical rearrangement from the chemisorbed reactant state than the cyclopropanes would.

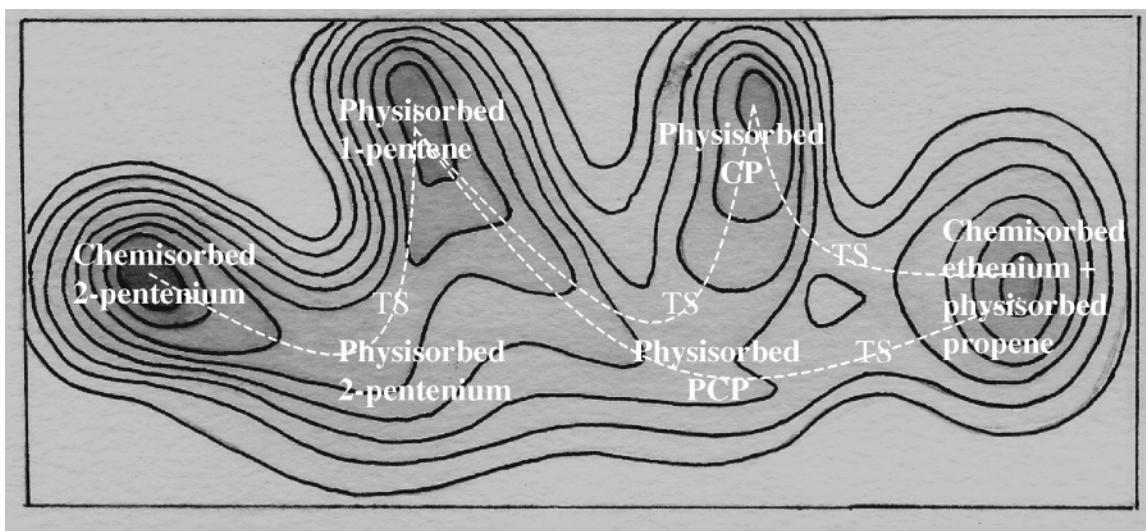
**Fig. 10.** Transition-state sketches for the scission (cracking) steps on  $\text{AlHCl}_3^-$ : (a) from a chemisorbed pentenium ion; (b) from a physisorbed protonated dimethylcyclopropane. The dashed lines indicate bonds in the reactant, while the squiggly lines indicate bonds in the product.



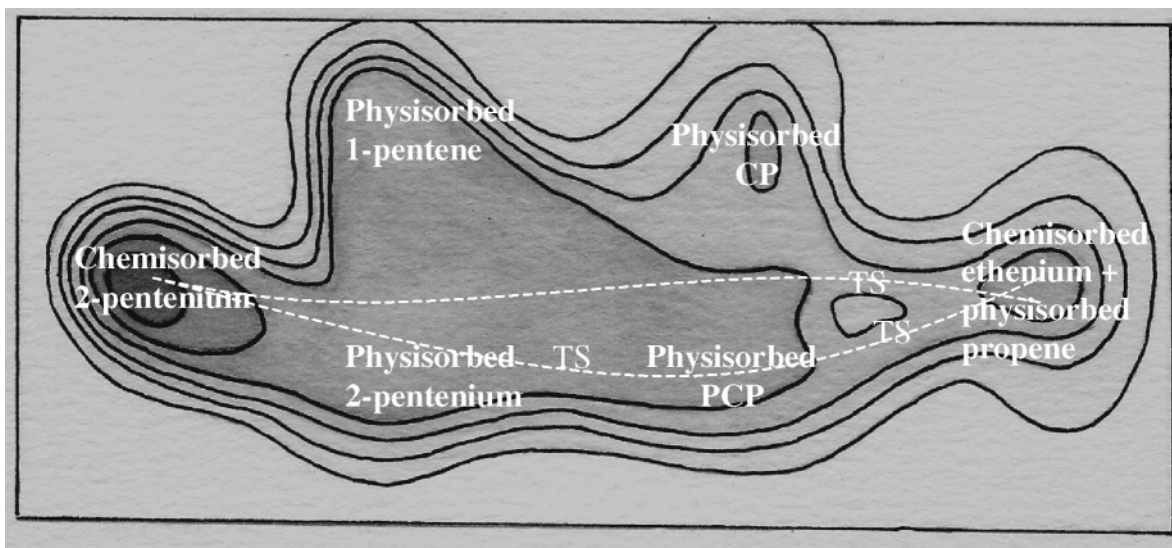
In Figure 11 ( $\text{AlH}_2(\text{OH})_2^-$  catalyst), although the intermediates are physisorbed neutral-pair complexes, the transition states for the steps are more like ion-pair ones, causing the reaction paths to be curved in this plot. Without the catalyst, the steps would have much larger reaction barriers as indicated by the high walls blocking the direct routes on this plot. Each step proceeds via a significant (40–50 kcal mol<sup>-1</sup>) energy barrier in the transition state before falling down into a well. This plot also helps to suggest that if the chemisorbed reactant has sufficient energy to overcome the first barrier, it might have sufficient excess energy and kinetic momentum to continue further down the channel towards complete  $\beta$  scission without having to fall down into either of the two potential wells for physisorbed neutral-pair intermediates.

In Fig. 12 ( $\text{AlHCl}_3^-$  catalyst), the biggest difference relative to Fig. 11 is that the energies of the ion-pair intermediates (the lower half of the plot) have dropped significantly

**Fig. 11.** Sketch of a plausible PES for  $\beta$  scission of the 2-pentenium ion on the  $\text{AlH}_2(\text{OH})_2^-$  catalyst, based on B3LYP/6-31G(d,p) stationary points. Each contour represents a rise of  $10 \text{ kcal mol}^{-1}$  from dark to light ( $1 \text{ cal} = 4.184 \text{ J}$ ). The bottom half of the figure represents ion-pair complexes, such that a vertical rise to the top half represents proton transfer to the catalyst to obtain neutral-pair complexes. Note that all four transition states have a great deal of ion-pair character, as indicated by their location in the bottom half of the diagram.



**Fig. 12.** Sketch of a plausible PES for  $\beta$  scission of the 2-pentenium ion on the  $\text{AlHCl}_3^-$  catalyst, based on B3LYP/6-31G(d,p) stationary points. Each contour represents a rise of  $10 \text{ kcal mol}^{-1}$  from dark to light ( $1 \text{ cal} = 4.184 \text{ J}$ ). The bottom half of the figure represents ion-pair complexes, such that a vertical rise to the top half represents proton transfer to the catalyst to obtain neutral-pair complexes. The minimum for the physisorbed ion-pair complex  $\text{PCP}^+/\text{AlHCl}_3^-$  cannot be seen on this scale, owing to the flatness of the surface in the physisorbed regions.



relative to the neutral-pair intermediates, and so much so that the energies of ion-pair vs. neutral-pair structures have become competitive. The  $\beta$ -scission reaction proceeds along a wide, flat path before rising over a transition state late in the reaction.

We think these plots demonstrate that the qualitative differences between the two mechanisms are due to the lowering of the ion-pair regions of the PES relative to the neutral-pair ones, in substituting chloride for hydroxide on the catalyst. This lowering is due to the lowered proton affinity of

the catalyst; we computed the proton affinities of our two catalysts with B3LYP/6-31G(d,p), and they are  $338 \text{ kcal mol}^{-1}$  for  $\text{AlH}_2(\text{OH})_2^-$  and  $276 \text{ kcal mol}^{-1}$  for  $\text{AlHCl}_3^-$ . For those concerned with the imbalance of the number of hydrides on each catalyst, this effect is minor; we calculated the proton affinity of  $\text{AlH}_2\text{Cl}_2^-$  and obtained  $285 \text{ kcal mol}^{-1}$ . Hence, since the catalysts are virtually identical in size, the lower basicity (or proton affinity) of chlorine atoms vs. oxygen atoms is the cause of the mechanistic differences here. This demonstration of catalyst basicity effects on mecha-

nism meshes nicely with our earlier study on the protolysis of hexane (23), which demonstrated that catalyst acidity could cause qualitative differences in its mechanism.

### Revisiting previous $\beta$ -scission modelling work

Frash et al. (FKRS) (24) studied the  $\beta$  scission of chemisorbed 1-butenium and 2-pentenium ions on two model zeolite fragments,  $\text{AlH}_2(\text{OH})_2^-$  and  $\text{AlH}_2(\text{OSiH}_3)_2^-$ , using HF/6-31G(d) and B3LYP/6-31G(d) geometry optimizations. The B3LYP results with the  $\text{AlH}_2(\text{OH})_2^-$  fragment were the ones we took and greatly extended by adding five transition states to their one on this PES. FKRS stated that on this PES the “alkoxy” (chemisorbed) reactant first converts to a CP intermediate before performing the scission step; we have convinced ourselves that this is not correct, and that minimum energy ascension of the chemisorbed reactant leads formally to a physisorbed propene intermediate, which can then isomerize to CP or directly perform  $\beta$  scission itself. FKRS were likely misled by the 1-butenium PES for which they did find a transition state from the chemisorbed reactant directly to CP, but the difference may be due to the ability of 2-pentenium ion to lose a nearby methyl proton upon ascension, which 1-butenium ion cannot do. FKRS also expressed surprise that the B3LYP PES produced a two-step pathway, because their HF/6-31G(d) PES produced a one-step, direct  $\beta$  scission from chemisorbed 2-pentenium ion. Our Fig. 11 may help to understand the qualitative difference; it is conceivable that a different level of theory might produce a slight shift of the contours around 40 kcal mol<sup>-1</sup> to produce a direct connection from chemisorbed reactant all the way to chemisorbed product. FKRS seemed to prefer the HF results over the B3LYP results, despite B3LYP being the higher level of theory; given that the difference may only be a subtle change in the PES, we suggest that the qualitative difference should not be worrisome, and that a proper description of the mechanism should include pathways connecting all four minima of Fig. 11 via carbenium ion paths.

Hay et al. (25) modelled the  $\beta$ -scission reaction of 2-pentenium ion with the zeolite fragment  $\text{AlH}_2(\text{OSiH}_3)_2^-$ , using HF/6-31G(d) optimized structures and B3LYP/6-31G(d) energies computed at the HF structures. They state the path as going from physisorbed pentene to chemisorbed 2-pentenium ion and then directly to products, in disagreement with our results. However, the direct  $\beta$  scission from the chemisorbed reactant does agree with the HF/6-31G(d) results of FKRS (24) with a different fragment model, and hence we merely comment that HF theory is being consistent in this matter, but that B3LYP optimizations present a different picture.

Svelle et al. (26) modelled the dimerization of linear alkenes with the zeolite fragment  $\text{Al}(\text{OH})(\text{OSiH}_3)_3^-$  (the active catalyst had an extra proton on an O atom between Al and a Si atom) using B3LYP/6-31G(d) optimizations and higher level single-point energies at these geometries.  $\beta$  Scission is the same reaction in the opposite direction. They refer to  $\pi$  and  $\sigma$  complexes, which in our language are physisorbed alkene and chemisorbed species, respectively. They refer to concerted vs. stepwise pathways; their stepwise hypothesis features a  $\beta$ -scission step between chemisorbed states, while the concerted hypothesis features a  $\beta$ -scission step between physisorbed states. However, despite

showing figures of these hypotheses in their Results section, they admit to never finding chemi- to chemi- $\beta$ -scission steps, as well as discovering some CP minima upon testing their transition states. Their results in fact agree with ours that  $\beta$  scission starts from various physisorbed states and not chemisorbed ones. Their finding of a  $\beta$ -scission step between two physisorbed states intrigued us, since we could not find such a step with our model system, so we tried some further calculations. We found that this step is unusually sensitive to the fragment model used: such a step exists for our pentene intermediate (1-pentene  $\rightarrow$  propene + ethene) on the activated  $\text{Al}(\text{OH})(\text{OSiH}_3)_3^-$  fragment of Svelle et al., but not on activated  $\text{Al}(\text{OH})_4^-$  or  $\text{AlH}_2(\text{OH})_2^-$ .

### Chemisorbed or physisorbed reactants?

Conventional organic chemistry states that cationic  $\beta$  scission starts from a carbenium ion. After the initial computations of Kazansky and co-worker (10, 11), it has been assumed (12, 24) that this  $\beta$  scission (on a zeolite) starts with the carbenium ion in an alkoxy (chemisorbed) state. However, this is not necessarily true. Our thorough calculations with  $\text{AlH}_2(\text{OH})_2^-$  suggest that *physisorbed alkenes* can undergo  $\beta$  scission directly, without having to become chemisorbed ions (see Fig. 11). Furthermore, even though the  $\beta$ -scission step immediately results in a chemisorbed primary carbenium ion on  $\text{AlH}_2(\text{OH})_2^-$ , Svelle et al. (26) with  $\text{Al}(\text{OH})(\text{OSiH}_3)_3^-$  found a  $\beta$  scission that resulted in physisorbed products. Hence, chemisorbed ions are not a requirement for the initial or final state in the cracking step. It might be better to think of the chemisorbed state as a “storage” state of alkenes or carbenium ions, rather than the active form of the reactant species.

### Conclusions

At the B3LYP/6-31G(d,p) level of theory, catalyzed  $\beta$  scission of a secondary carbenium ion is qualitatively different on  $\text{AlHCl}_3^-$  than it is on  $\text{AlH}_2(\text{OH})_2^-$ , which is due only to the differing basicities of Cl and O atoms. On the  $\text{AlH}_2(\text{OH})_2^-$  catalyst, the stable physisorbed intermediates are neutral alkenes or alkylcyclopropanes (CP). On the less basic  $\text{AlHCl}_3^-$  catalyst, however, the intermediates are protonated alkylcyclopropanes (PCP).

Although these chosen catalysts are not models of true ionic liquids or aluminosilicate zeolites, they happened to produce the same qualitative intermediates (ion pair vs. neutral pair) that are thought to exist in these two true systems.

With  $\text{AlHCl}_3^-$ ,  $\beta$  scission can occur directly from the chemisorbed state, or occur via a barely stable ion-pair intermediate. With  $\text{AlH}_2(\text{OH})_2^-$ , the scission step does not start from the chemisorbed state, but from physisorbed neutral-pair states, although trajectories with small excess energies and reaction momentum could achieve  $\beta$  scission from chemisorbed states.

### Acknowledgments

This research was funded by the Natural Sciences and Engineering Research Council of Canada (NSERC) and the Canada Foundation for Innovation (CFI). The Laboratory of Computational Discovery (University of Regina, Regina,

Saskatchewan) is thanked for computational resources. D. Roettger is thanked for drawing the contour plots.

## References

1. L. Xiao, K.E. Johnson, and R.G. Treble. *J. Mol. Catal. A*, **214**, 121 (2004).
2. G.A. Olah, Y. Halpern, J. Shen, and Y.K. Mo. *J. Am. Chem. Soc.* **95**, 4960 (1973).
3. Y. Zhao, G.R. Bamwenda, and B.W. Wojciechowski. *J. Catal.* **142**, 465 (1993).
4. W.O. Haag and R.M. Dessau. *Proc. Int. Congr. Catal.* 8th, **2**, 305 (1985).
5. J. Engelhardt and W.K. Hall. *J. Catal.* **151**, 1 (1995).
6. S.T. Sie. *In Handbook of heterogeneous catalysis*. Vol. 4. Edited by G. Ertl, H. Knozinger, and J. Weitkamp. VCH, Weinheim, Germany. 1997. p. 1998.
7. J.F. Haw. *Phys. Chem. Chem. Phys.* **4**, 5431 (2002).
8. G.M. Kramer, G.B. McVicker, and J.J. Ziemak. *J. Catal.* **92**, 355 (1985).
9. J.F. Haw, B.R. Richardson, I.S. Oshiro, N.D. Lazo, and J.A. Speed. *J. Am. Chem. Soc.* **111**, 2052 (1989).
10. V.B. Kazansky and I.N. Senchenya. *Kinet. Katal.* **28**, 566 (1987).
11. V.B. Kazansky. *Acc. Chem. Res.* **24**, 379 (1991).
12. V.B. Kazansky. *Catal. Today*, **51**, 419 (1999).
13. M.V. Frash and R.A. van Santen. *Top. Catal.* **9**, 191 (1999).
14. T. Demuth, X. Rozanska, L. Benco, J. Hafner, R.A. van Santen, and H. Toulhoat. *J. Catal.* **214**, 68 (2003).
15. J.L. White, L.W. Beck, and J.F. Haw. *J. Am. Chem. Soc.* **114**, 6182 (1992).
16. J.B. Nicholas, T. Xu, and J.F. Haw. *Top. Catal.* **6**, 141 (1998).
17. W. Song, J.B. Nicholas, and J.F. Haw. *J. Am. Chem. Soc.* **123**, 121 (2001).
18. I.I. Ivanova, E.B. Pomakhina, A.I. Rebrov, and E.G. Derouane. *Top. Catal.* **6**, 49 (1998).
19. E.G. Derouane, H. He, S.B. Derouane-Abd Hamid, D. Lambert, and I. Ivanova. *Catal. Lett.* **58**, 1 (1999).
20. E.G. Derouane, H. He, S.B. Derouane-Abd Hamid, D. Lambert, and I. Ivanova. *J. Mol. Catal. A: Chem.* **158**, 5 (2000).
21. A.G. Stepanov, M.V. Luzgin, V.N. Romannikov, and K.I. Zamaraev. *Catal. Lett.* **24**, 271 (1994).
22. A.G. Stepanov, M.V. Luzgin, V.N. Romannikov, V.N. Sidelnikov, and E.A. Paukshtis. *J. Catal.* **178**, 466 (1998).
23. K.C. Hunter, C. Seitz, and A.L.L. East. *J. Phys. Chem. A*, **107**, 159 (2003).
24. M.V. Frash, V.B. Kazansky, A.M. Rigby, and R.A. van Santen. *J. Phys. Chem. B*, **102**, 2232 (1998).
25. P.J. Hay, A. Redondo, and Y. Guo. *Catal. Today*, **50**, 517 (1999).
26. S. Svelle, S. Kolboe, and O. Swang. *J. Phys. Chem. B*, **108**, 2953 (2004).
27. D.E. Brown, D.J. Moffatt, and R.A. Wolkow. *Science (Washington, D.C.)*, **279**, 542 (1998).
28. A.D. Becke. *J. Chem. Phys.* **98**, 5648 (1993).
29. C. Lee, W. Yang, and R.G. Parr. *Phys. Rev. B*, **37**, 785 (1988).
30. M.J. Frisch, G.W. Trucks, H.B. Schlegel, G.E. Scuseria, M.A. Robb, J.R. Cheeseman, V.G. Zakrzewski, J.A. Montgomery, R.E. Stratmann, J.C. Burant, S. Dapprich, J.M. Millam, A.D. Daniels, K.N. Kudin, M.C. Strain, O. Farkas, J. Tomasi, V. Barone, M. Cossi, R. Cammi, B. Mennucci, C. Pomelli, C. Adamo, S. Clifford, J. Ochterski, G.A. Petersson, P.Y. Ayala, Q. Cui, K. Morokuma, D.K. Malick, A.D. Rabuck, K. Raghavachari, J.B. Foresman, J. Cioslowski, J.V. Ortiz, B.B. Stefanov, G. Liu, A. Liashenko, P. Piskorz, I. Komaromi, R. Gomperts, R.L. Martin, D.J. Fox, T. Keith, M.A. Al-Laham, C.Y. Peng, A. Nanayakkara, C. Gonzalez, M. Challacombe, P.M.W. Gill, B.G. Johnson, W. Chen, M.W. Wong, J.L. Andres, M. Head-Gordon, E.S. Replogle, and J.A. Pople. GAUSSIAN 98. Revision A.9 [computer program]. Gaussian, Inc., Pittsburgh, Pennsylvania. 1998.
31. PQS 3.0 [computer program]. Parallel Quantum Solutions, Fayetteville, Arkansas. 2004.
32. J. Baker. *J. Comput. Chem.* **7**, 385 (1986).
33. K.C. Hunter. M.Sc. thesis, University of Regina, Regina, Saskatchewan. 2002.
34. D.W. Chandler and K.E. Johnson. *J. Inorg. Chem.* **38**, 2050 (1999).
35. J.L. Campbell and K.E. Johnson. *J. Am. Chem. Soc.* **117**, 7791 (1995).